2026 极端核物质前沿研讨会
April 24 -28 WORKSHOP ON EXTREME NUCLEAR MATTER FRONTIERS

Heavy-quark transport across the QCD crossover driven by a lattice-constrained in-medium potential

Shuang Li (李 双)
China Three Gorges University (CTGU)

+ in collaboration with Sa Wang (王 洒)、Fei Sun (孙 飞)
+ based on: 2604.10889; PRD 112, 116001 (2025)

Outline

- **Introduction: Heavy quarks as probes of QGP**
- **Theoretical Framework: From Static Potential to Scattering Dynamics**
- **Numerical Results: dE/dz, $\hat{q}$, $2\pi T D_s$**
- **Summary and Outlook**

Heavy quarks (HQ) as probes of QGP

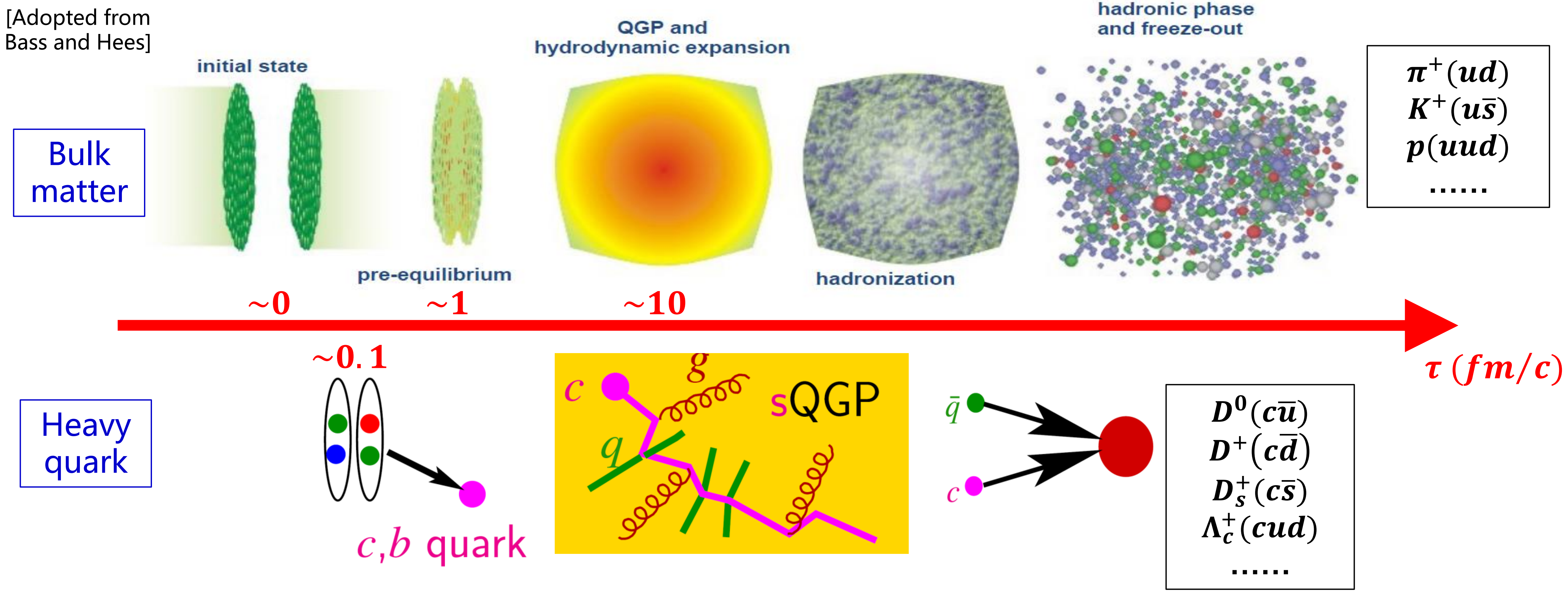

- $m_Q \gg \Lambda_{QCD}$: their initial production can be well described by pQCD
- $m_Q \gg T$: thermal abundance in QGP is negligible ~ final multiplicity set by the initial hard production
- $m_Q \gg gT$: many soft scatterings necessary to change significantly the momentum of HQ ~ Brownian motion

HQ transport at different temperature scales

- **Weak-coupling** approach (high-temperature limit)
  - ✓ The medium is a weakly-coupled gas of quarks and gluons (wQGP)
  - ✓ Dominated by few-body scatterings with Debye screening $m_D \sim gT \ll T$
  - ✓ LO pQCD provides a logarithmic dependence of energy loss

J. Lou, SL, et al., Phys. Rev. D 112, 116001 (2025)

  - ✓ $2\pi T D_s \sim 30$ near T_c (relatively large)

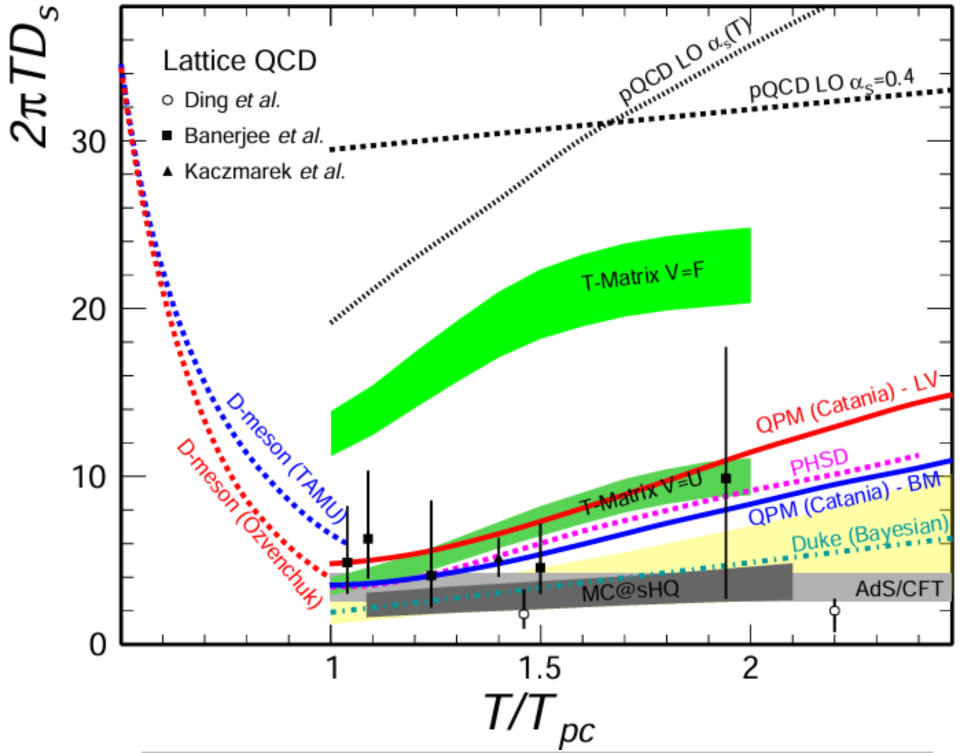

M. He, H. van Hees, and R. Rapp, Prog. Part. Nucl. Phys. 130, 104020 (2023)

HQ transport at different temperature scales

- **Strong-coupling**
  - ✓ $g(T)$ is large and $\alpha_s = g^2/(4\pi)$ no longer converges
  - ✓ Remnants of confinement and chiral symmetry effects emerge
  - ✓ Lattice QCD extractions show $2\pi T D_s \sim 1$ near T_c (much smaller than pQCD)
  - ✓ **Non-perturbative contributions** are indispensable to describe the medium response

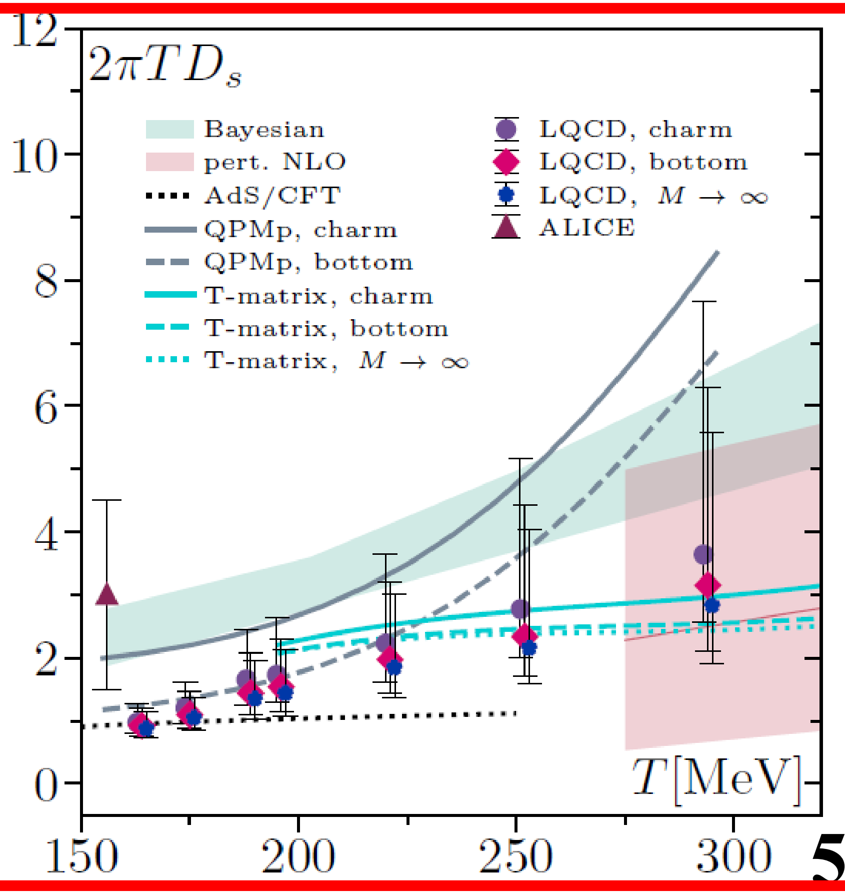

D. Bollweg, et al., JHEP 09 (2025) 180

Bridging the scales: boundary-free interaction kernel

- **Current issue: artificial "soft-hard" separation (arbitrary cutoff t^*)**
- **Our objective: seamless transition from UV to IR regimes**
- **Unified mapping: static potential → real-time scattering kernel**
  - ✓ Short-range: Yukawa screening
  - ✓ Long-range: String tension
- **Building boundary-free & scale-independent framework: parameters rigorously constrained by lattice QCD**

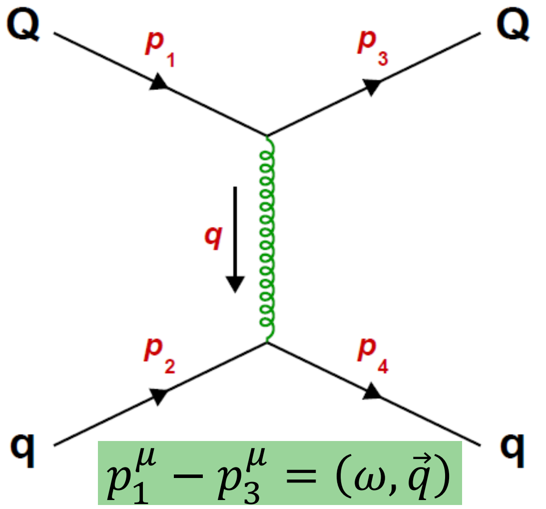

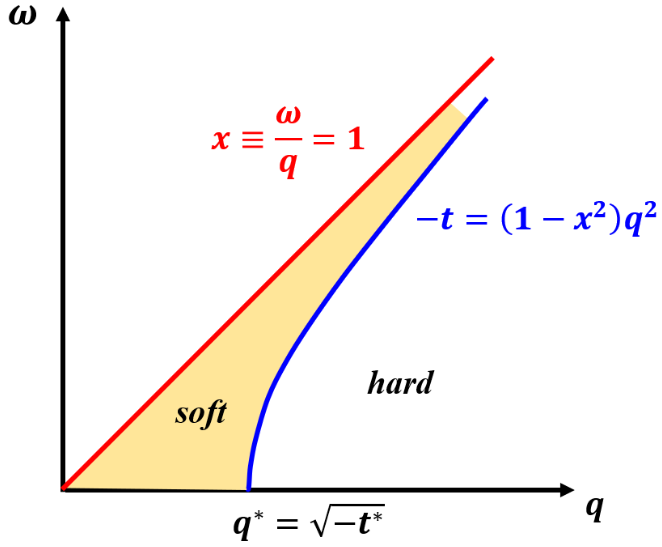

J. Peng, SL, et al., 2510.10294;
Phys. Rev. D 109, 096028 (2024);

Potential scattering framework

- In vacuum, the heavy quark potential is

E. Eichten, et al., Phys. Rev. D 17, 3090 (1978)

$$V_{\mathrm{vac}}(r,0) = -\frac{\tilde{\alpha}_s}{r} + \sigma r + V_0,$$

Coulombic part **linear confining part**

and in medium $V(r,T) = V_{\mathrm{Y}}(r,T) + V_{\mathrm{S}}(r,T) + V_0$

$$V_{\mathrm{Y}}(r,T) = -\tilde{\alpha}_s\left(M_{\mathrm{D}} + \frac{e^{-M_{\mathrm{D}}r}}{r}\right),$$

Yukawa term

$$V_{\mathrm{S}}(r,T) = \frac{2\sigma}{M_{\mathrm{D}}} - \frac{\sigma}{M_{\mathrm{D}}}e^{-M_{\mathrm{D}}r}\left(2 + M_{\mathrm{D}}r\right)$$

String term

the effective screening mass M_D is extracted by fitting the lattice data which is then parametrized using

$$M_{\mathrm{D}}(T) = m_{\mathrm{D}}(T) + \frac{N_c g^2 T}{4\pi}\ln\left[\frac{m_{\mathrm{D}}(T)}{g^2 T}\right] + \kappa_1 g^2 T + \kappa_2 g^3 T$$

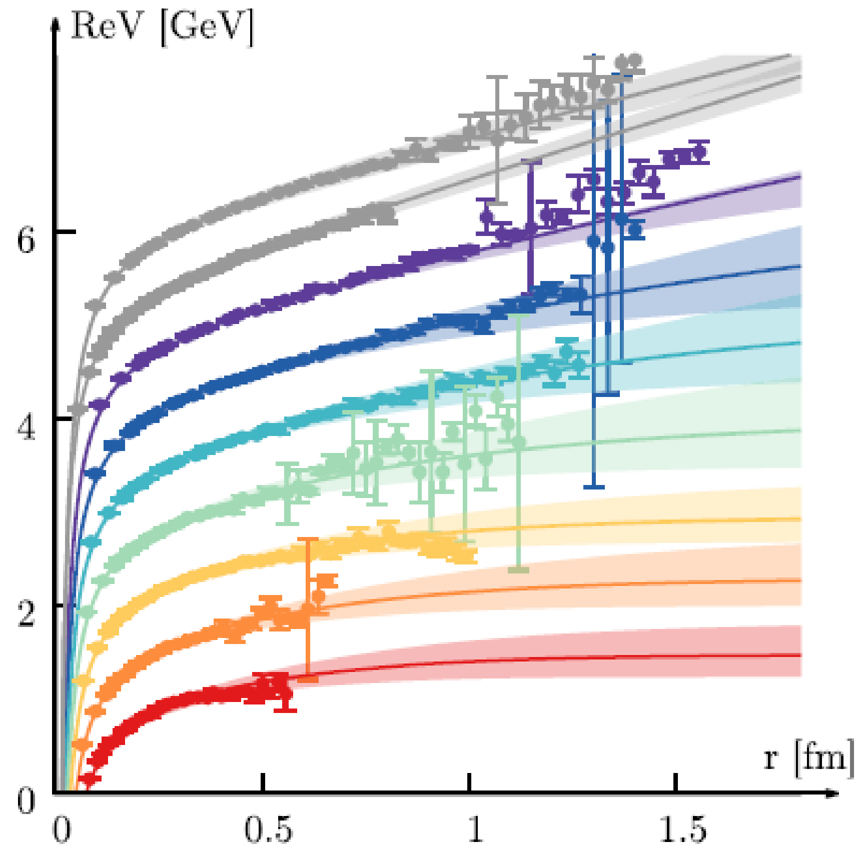

D. Lafferty and A. Rothkopf, Phys. Rev. D 101, 056010 (2020)

Potential scattering framework

- The potential in momentum-space

$$\tilde{V}(q,T) = \tilde{V}_{\mathrm{Y}}(q,T) + \tilde{V}_{\mathrm{S}}(q,T) + (2\pi)^3 V_{\mathrm{const}}\delta^{(3)}(\vec{q}).$$

$$\tilde{V}_{\mathrm{Y}}(q,T) = -\frac{4\pi\tilde{\alpha}_s}{q^2 + M_{\mathrm{D}}^2},$$

$$\tilde{V}_{\mathrm{S}}(q,T) = -8\pi\sigma\frac{q^2 + 5M_{\mathrm{D}}^2}{(q^2 + M_{\mathrm{D}}^2)^3}.$$

- The potential as an effective gluon propagator

$$\begin{aligned} i\mathcal{M} =& \mathcal{M}_{\mathrm{Y}} + \mathcal{M}_{\mathrm{S}} \\ =& \bar{u}(P_3)\gamma^{\mu}u(P_1)\tilde{V}_{\mathrm{Y}}\bar{u}(P_4)\gamma_{\mu}u(P_2) \\ &+ \bar{u}(P_3)u(P_1)\tilde{V}_{\mathrm{S}}\bar{u}(P_4)u(P_2), \end{aligned}$$

W.-J. Xing, G.-Y. Qin, and S. Cao, Phys. Lett. B 838, 137733 (2023)
F. Riek and R. Rapp, Phys. Rev. C 82, 035201 (2010)

Potential scattering framework

- For $Q + q$

$$\overline{|\mathcal{M}_{Qq}|^2}_{\mathrm{Y}} = \frac{64\pi^2\alpha_s^2}{9}\frac{\tilde{s}^2 + \tilde{u}^2 + 2m_1^2 t}{(t - M_{\mathrm{D}}^2)^2}$$

$$\overline{|\mathcal{M}_{Qq}|^2}_{\mathrm{S}} = \frac{1}{N_c^2 - 1}(t^2 - 4m_1^2 t)\left[\frac{8\pi\sigma(t - 5M_{\mathrm{D}}^2)}{(t - M_{\mathrm{D}}^2)^3}\right]^2$$

$$\tilde{s} \equiv s - m_1^2$$

$$\tilde{u} \equiv u - m_1^2$$

- For $Q + g$

$$\begin{aligned}\overline{|\mathcal{M}_{Qg}|^2}_{\mathrm{Y}} =& 16\pi^2\alpha_s^2\left[2\frac{-\tilde{s}\tilde{u}}{(t - M_{\mathrm{D}}^2)^2} + \frac{4}{9}\frac{-\tilde{s}\tilde{u} + 2m_1^2(s + m_1^2)}{\tilde{s}^2}\right.\\ &+ \frac{4}{9}\frac{-\tilde{s}\tilde{u} + 2m_1^2(m_1^2 + u)}{\tilde{u}^2} + \frac{1}{9}\frac{m_1^2(4m_1^2 - t)}{-\tilde{s}\tilde{u}}\\ &\left.+ \frac{-\tilde{s}\tilde{u} + m_1^2(s - u)}{(t - M_{\mathrm{D}}^2)\tilde{s}} - \frac{-\tilde{s}\tilde{u} - m_1^2(s - u)}{-(t - M_{\mathrm{D}}^2)\tilde{u}}\right],\end{aligned}$$

$$\overline{|\mathcal{M}_{Qg}|^2}_{\mathrm{S}} = \frac{C_A}{C_F}\frac{1}{N_c^2 - 1}(t^2 - 4m_1^2 t)\left[\frac{8\pi\sigma(t - 5M_{\mathrm{D}}^2)}{(t - M_{\mathrm{D}}^2)^3}\right]^2$$

Potential scattering framework

- The total interaction rate for a heavy quark scattering off the surrounding thermal medium partons is

$$\Gamma(E_1,T)=\sum_{i=q,g}\Gamma_i(E_1,T)=\frac{1}{2E_1}\sum_{i=q,g}\int\frac{d^3\vec{p}_2}{(2\pi)^3 2E_2}n_i(E_2,T)\int\frac{d^3\vec{p}_3}{(2\pi)^3 2E_3}\int\frac{d^3\vec{p}_4}{(2\pi)^3 2E_4}\overline{|\mathcal{M}^2|}_{Qi}(2\pi)^4\delta^{(4)}(\Sigma P)$$

- The scale independent energy loss per unit path length and the momentum diffusion coefficients are

$$-\frac{dE}{dz}=\int d^3\vec{q}\frac{d\Gamma}{d^3\vec{q}}\frac{\omega}{v_1}=\frac{1}{256\pi^3 p_1^2}\sum_{i=q,g}\int_0^\infty dp_2 E_2 n_i(E_2,T)\int_{-1}^{1}d(\cos\psi)\int_{t_{min}}^{0}dt\frac{b}{a^3}\overline{|\mathcal{M}_{Qi}^2|},$$

$$\kappa_T=\frac{1}{2}\int d^3\vec{q}\frac{d\Gamma}{d^3\vec{q}}\vec{q}_T^{\,2}=\frac{1}{256\pi^3 p_1^3 E_1}\sum_{i=q,g}\int_0^\infty dp_2 E_2 n_i(E_2,T)\int_{-1}^{1}d(\cos\psi)\int_{t_{min}}^{0}dt\ \mathcal{A}\overline{|\mathcal{M}_{Qi}^2|},$$

$$\kappa_L=\int d^3\vec{q}\frac{d\Gamma}{d^3\vec{q}}q_L^2=\frac{1}{256\pi^3 p_1^3 E_1}\sum_{i=q,g}\int_0^\infty dp_2 E_2 n_i(E_2,T)\int_{-1}^{1}d(\cos\psi)\int_{t_{min}}^{0}dt\ \mathcal{B}\overline{|\mathcal{M}_{Qi}^2|},$$

$$\hat{q}=\frac{2\kappa_T}{v}$$

$$2\pi T D_s=\frac{4\pi}{\kappa/T^3}$$

$$\kappa\approx\kappa_T\approx\kappa_L\ (v=0)$$

Collisional energy loss

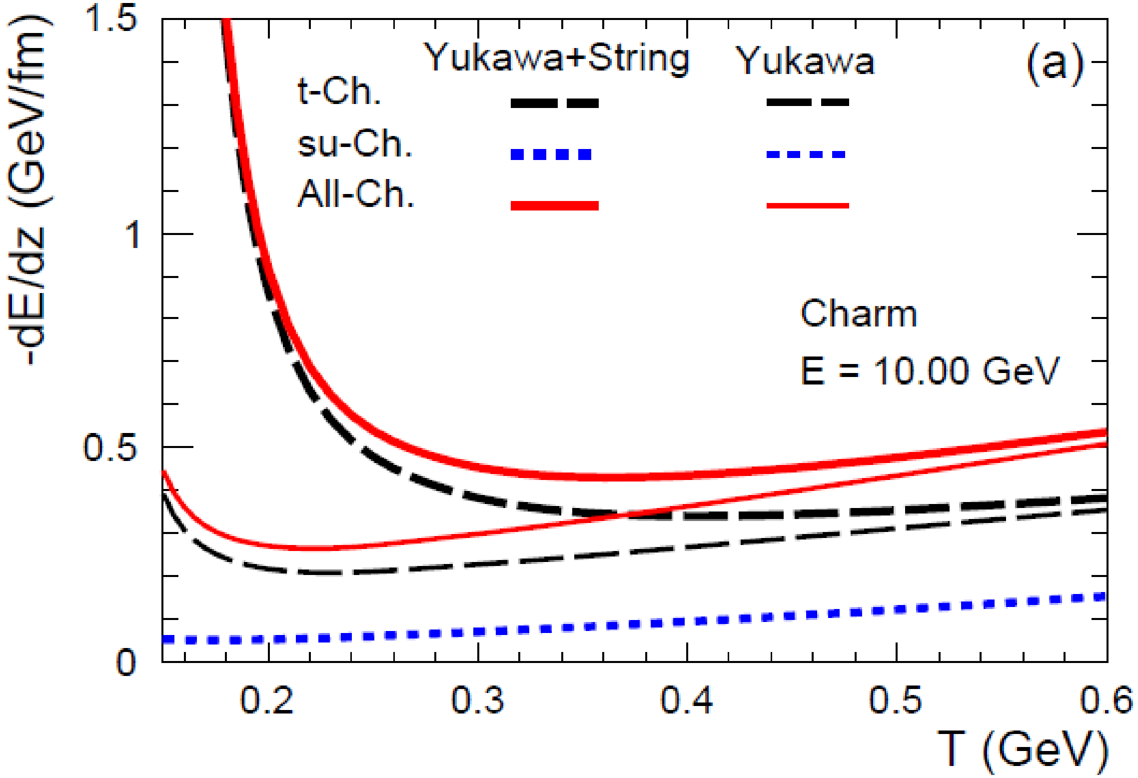

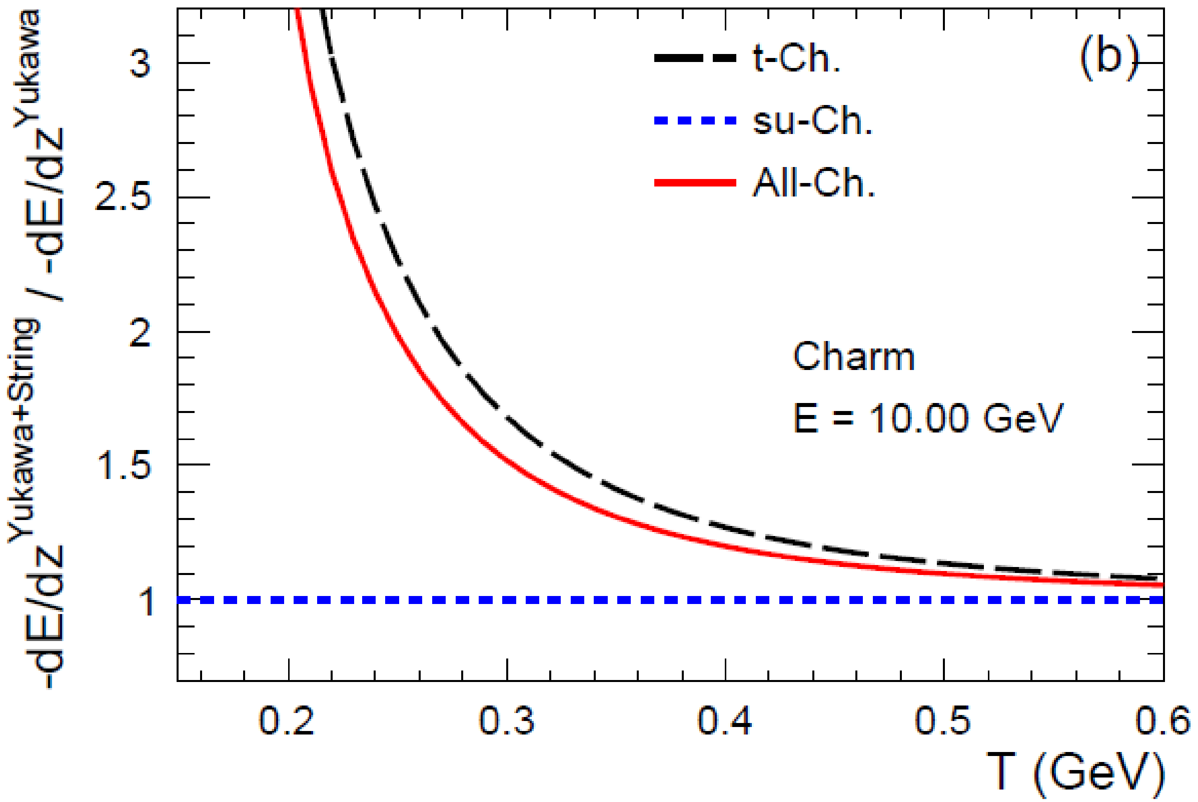

- Low-T enhancement: strong enhancement of energy loss near $T_c = 172.5\ \mathrm{MeV}$, fundamentally driven by long-range string interactions
- High- T asymptotics: seamless transition to pure Yukawa (pQCD) behavior as the non-perturbative string tension dynamically melts

Jet transport coefficient

- Kinematic penetration: at ultra-high energies ($E = 100$ GeV), deeply penetrating hard scatterings dominate; string effects become negligible

- Near-T_c peak structure: predicts a prominent peak, maintaining qualitative agreement with JETSCAPE ($E = 100$ GeV) and Jet Collaboration ($E = 10$ GeV)

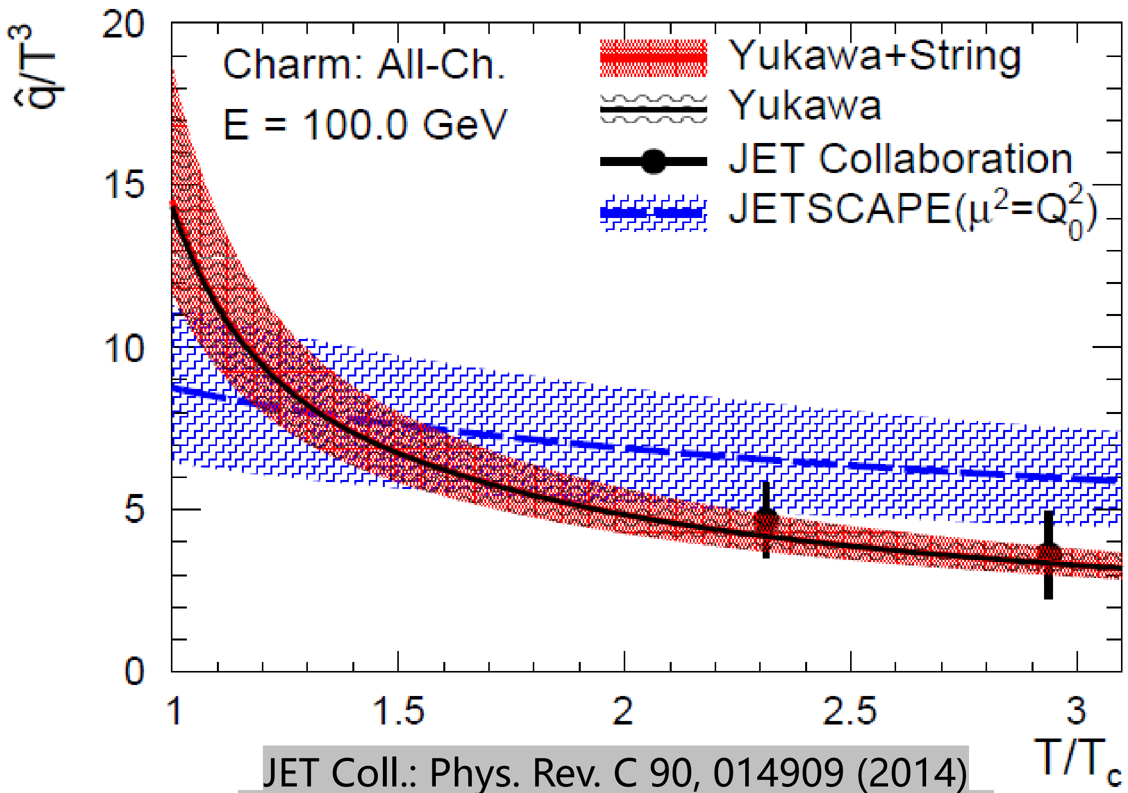

JET Coll.: Phys. Rev. C 90, 014909 (2014)
JETSCAPE: Phys. Rev. C 111, 054913 (2025)

- High-T deviation: underestimation at high temperatures explicitly highlights the necessity of incorporating inelastic radiative processes (LPM effect) in future updates

Momentum diffusion coefficient

- The perturbative gap: the pure Yukawa baseline severely underestimates the interaction; inclusion of the string term captures the missing opacity near T_c

- Consistency with T-matrix: the dynamically generated enhancement exhibits quantitative agreement with non-perturbative T-matrix resummation results

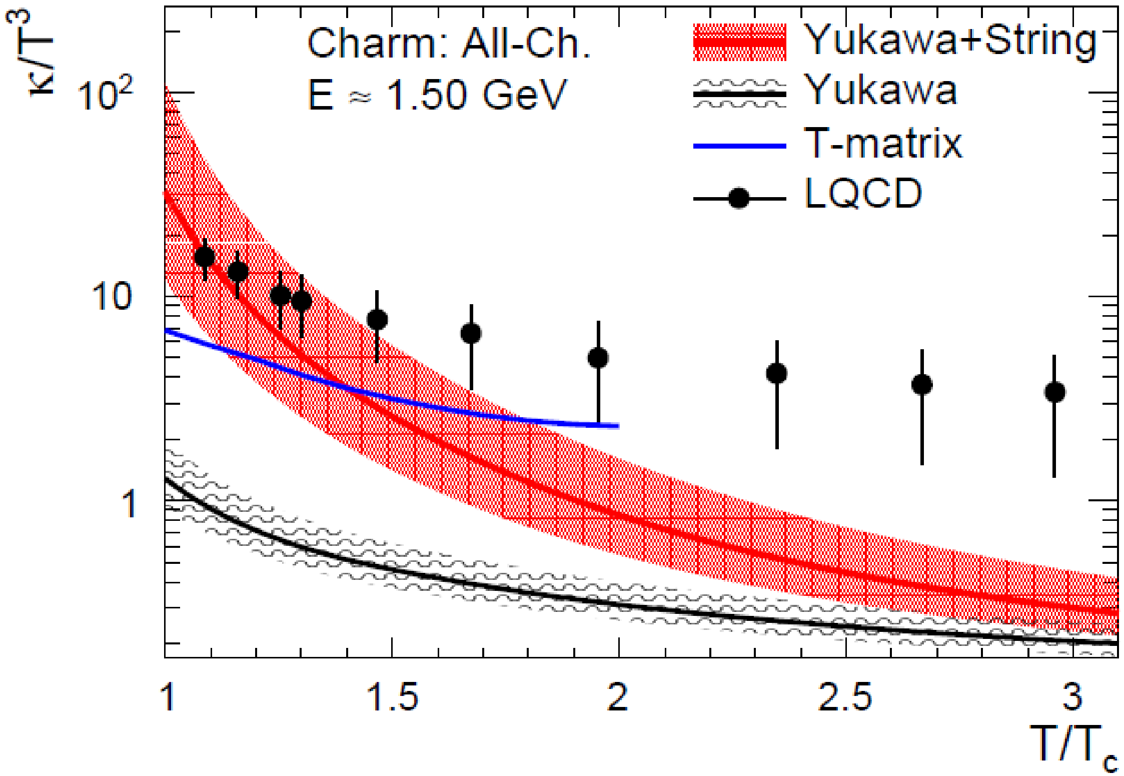

- Lattice validation: yields remarkable quantitative agreement with the latest HotQCD 2025 data in the critical crossover region

T-matrix: Phys. Rev. Lett. 110, 112301 (2013); Phys. Rev. C 82, 035201 (2010),
LQCD: JHEP 09, 180 (2025)

Spatial diffusion coefficient

- Strong-coupling minimum: predicts $2\pi T D_s \approx 0.5 - 1.7$ near T_c, showing striking consistency with both HotQCD 2025 data and T-matrix predictions

- Near-T_c universality: the near-degeneracy of charm and bottom diffusion reveals a universal, mass-insensitive scattering strength driven by the string tension

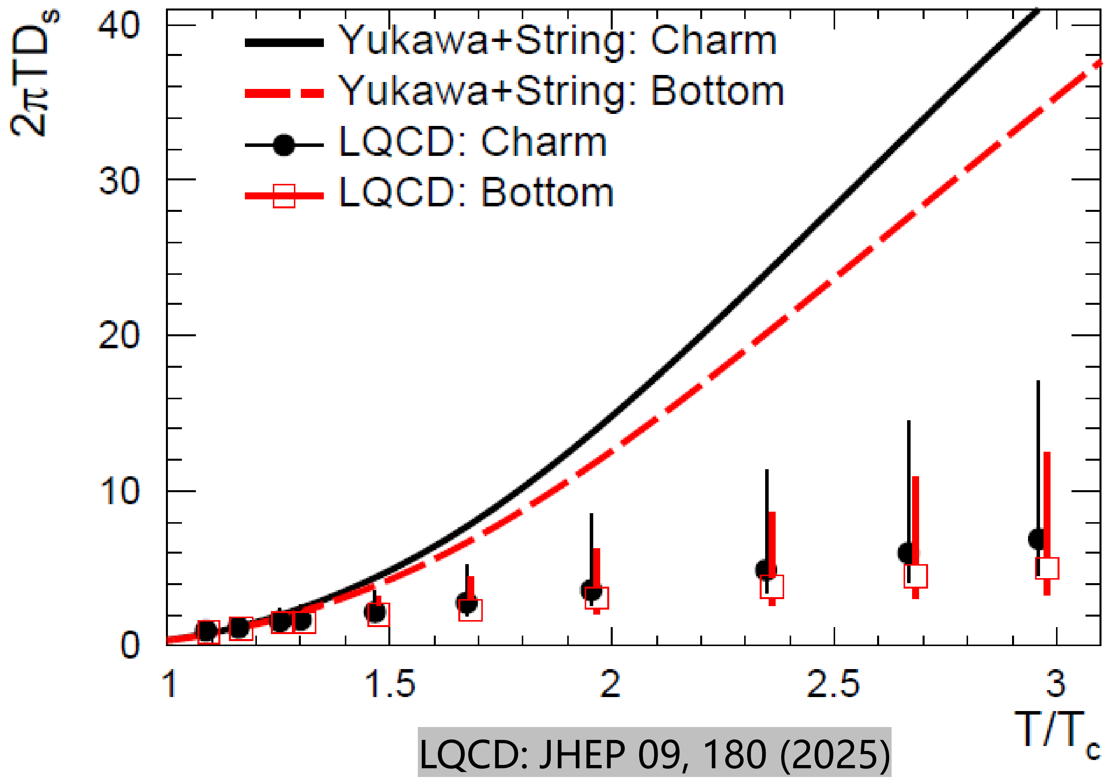

LQCD: JHEP 09, 180 (2025)

- Kinematic mass hierarchy: flavor separation cleanly emerges at higher temperatures, dynamically mirroring the mass-dependent trend observed in lattice data

Summary and outlook

- **We have developed a unified, lattice-constrained transport kernel, successfully eliminating the artificial soft-hard factorization scale**
  - ✓ Indispensable string effects: demonstrated that long-range confining correlations are the primary driving force behind the medium's extreme opacity near T_c
  - ✓ Validation: achieved striking quantitative agreement with the state-of-the-art HotQCD 2025 data, capturing both the magnitude and the mass hierarchy of D_s
  - ✓ Limits of elastic scattering: identified high-T deviations as a clear boundary for the static potential paradigm, pointing to the essential role of dynamical radiation

- **New paths forward for future work** (to phenomenology)
  - ✓ Implement these rigorous microscopic kernels into our macroscopic LGR (Langevin+Radiation) model to systematically evaluate heavy-flavor R_{AA} and v_2 across RHIC and LHC energies

Three Gorges Dam

Backup

$$\tilde{\alpha}_s = 0.406, \quad \sqrt{\sigma} = 0.495 \text{ GeV}, \quad V_0 = 2.356 \text{ GeV}$$

$$\kappa_1 = 0.686, \qquad \kappa_2 = -0.317.$$

$$(\kappa_1^{upp}, k_2^{upp}) = (0.862, -0.348)$$

$$(\kappa_1^{low}, k_2^{low}) = (0.421, -0.245)$$

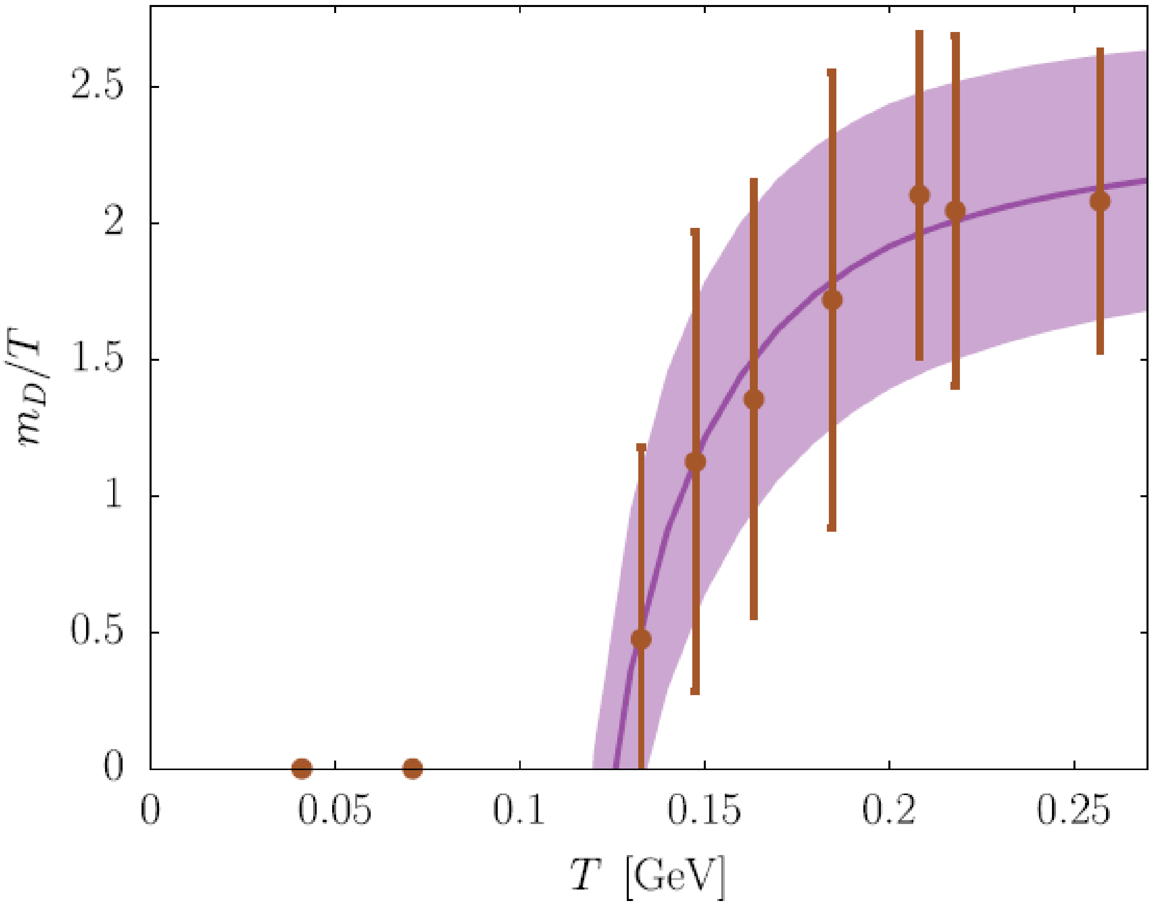

D. Lafferty and A. Rothkopf, Phys. Rev. D 101, 056010 (2020)

$$\mathcal{A} \equiv \frac{1}{a}\left[-\frac{m_1^2\left(D+2b^2\right)}{8{p_1}^2a^4}+\frac{E_1tb}{2{p_1}^2a^2}-t\left(1+\frac{t}{4{p_1}^2}\right)\right]$$

$$\mathcal{B} \equiv \frac{1}{a}\left[\frac{E_1^2\left(D+2b^2\right)}{4a^4}-\frac{E_1tb}{a^2}+\frac{t^2}{2}\right].$$

$$t_{min} = -\frac{\tilde{s}^2}{s}, \qquad a = \frac{\tilde{s}}{p_1},$$

$$b = -\frac{2t}{p_1^2}\left[E_1\tilde{s}-E_2\left(s+m_1^2\right)\right],$$

$$c = -\frac{t}{p_1^2}\left\{t\left[\left(E_1+E_2\right)^2-s\right]+4p_1^2p_2^2\sin^2\psi\right\},$$

$$D = -t\left(ts+\tilde{s}^2\right)\cdot\left(\frac{4E_2\sin\psi}{p_1}\right)^2.$$

$$n_B(E,T) = \left(e^{E/T}-1\right)^{-1},$$

$$n_F(E,T) = \left(e^{E/T}+1\right)^{-1}.$$

$$M_{\mathrm{D}}(T) = m_{\mathrm{D}}(T) + \frac{N_c g^2 T}{4\pi} \ln\left[\frac{m_{\mathrm{D}}(T)}{g^2 T}\right] + \kappa_1 g^2 T + \kappa_2 g^3 T, \tag{6}$$

where $m_{\mathrm{D}}(T)$ denotes the leading-order HTL Debye mass at vanishing chemical potential,

$$m_{\mathrm{D}}^2(T) = \left(\frac{N_c}{3} + \frac{N_f}{6}\right) g^2 T^2. \tag{7}$$

Here, $N_c = 3$ is the number of colors for $SU(N_c)$ symmetry and $N_f = 3$ is the number of quark flavors. The logarithmic term in Eq. (6) corresponds to the known next-to-leading-order correction [30, 31]. The running coupling $g(\Lambda) = g(2\pi T)$ is evaluated using the four-loop QCD beta function in the $\overline{\mathrm{MS}}$ scheme [32–34], initialized with $\Lambda_{\mathrm{QCD}}^{(5)} = 0.2145\,\mathrm{GeV}$ and matched across quark thresholds [35].

A crucial element of this framework is the rigorous separation between the static effective coupling $\tilde{\alpha}_s$, which intrinsically characterizes the lattice-extracted potential, and the dynamical running coupling $\alpha_s(\Lambda_{\text{hard}})$ that governs the interaction vertices in scattering processes. The static coupling $\tilde{\alpha}_s$ is fully embedded in the definition of the potential and must not be reintroduced at the interaction vertices to avoid unphysical double counting.

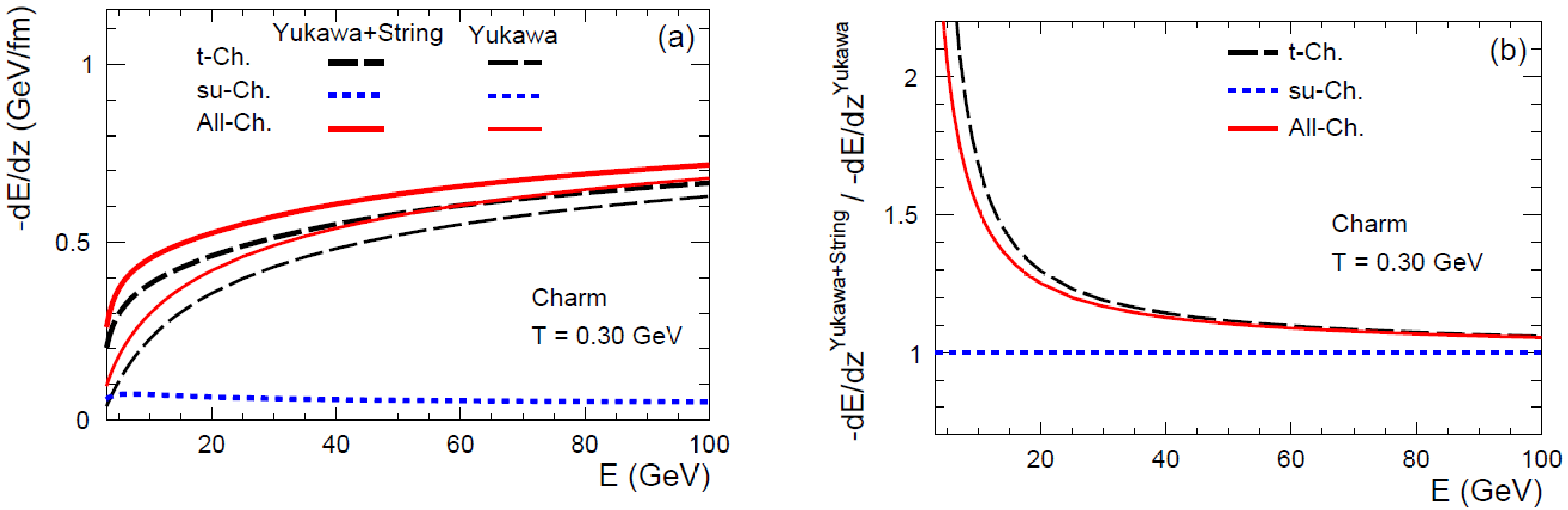
-dE/dz (GeV/fm)
Yukawa+String
Yukawa
t-Ch.
su-Ch.
All-Ch.
(a)
Charm
T = 0.30 GeV
E (GeV)
-dE/dz^Yukawa+String / -dE/dz^Yukawa
t-Ch.
su-Ch.
All-Ch.
(b)
Charm
T = 0.30 GeV
E (GeV)

Spatial diffusion coefficient

- Strong-coupling minimum: predicts $2\pi T D_s \sim 1$ near T_c, showing striking consistency with both HotQCD 2025 data and T-matrix predictions

- Near-T_c universality: the near-degeneracy of charm and bottom diffusion reveals a universal, mass-insensitive scattering strength driven by the string tension

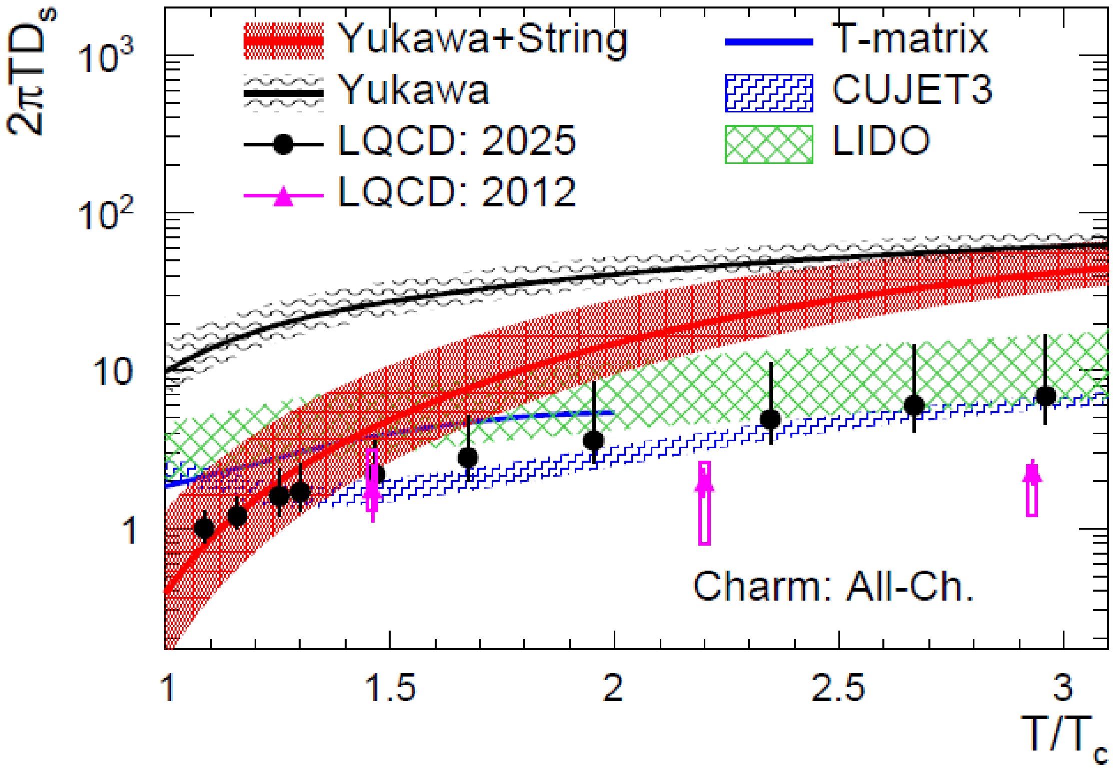

- Kinematic mass hierarchy: flavor separation cleanly emerges at higher temperatures, dynamically mirroring the mass-dependent trend observed in lattice data

LQCD: JHEP 09, 180 (2025); Phys. Rev. D 86, 014509 (2012); T-matrix: Phys. Rev. Lett. 110, 112301 (2013); Phys. Rev. C 82, 035201 (2010); CUJET3: Chin. Phys. C 43, 044101 (2019); LIDO: Phys. Rev. C 98, 064901 (2018)